

# Evidence for electronic phase separation between orbital orderings in $\text{SmVO}_3$

M.H. Sage<sup>1</sup>, G.R. Blake<sup>1</sup>, G.J. Nieuwenhuys<sup>2</sup>, and T.T.M. Palstra<sup>1\*</sup>

<sup>1</sup>*Solid State Chemistry Laboratory, Materials Science Centre,  
University of Groningen, Nijenborgh 4,  
9747 AG Groningen, The Netherlands.*

<sup>2</sup>*Kamerlingh Onnes Laboratorium, Leiden University,  
P.O. Box 9504, 2300 RA Leiden, The Netherlands.*

## Abstract

We report evidence for phase coexistence of orbital orderings of different symmetry in  $\text{SmVO}_3$  by high resolution X-Ray powder diffraction. The phase coexistence is triggered by an antiferromagnetic ordering of the vanadium spins near 130K, below an initial orbital ordering near 200K. The phase coexistence is the result of the intermediate ionic size of samarium coupled to exchange striction at the vanadium spin ordering.

PACS numbers: 61.10.Nz, 61.50.Ks, 71.70.Ej

Transition metal oxides with competing interactions have in recent years been shown to exhibit complex electronic behavior, in which different electronic phases may coexist. The competing interactions include the spin, charge and orbital degrees of freedom. The origin of the phase coexistence is often associated with a coupling of the electronic degrees of freedom to the lattice. Much interest has been triggered by colossal magneto-resistance materials where a metal-insulator transition involves a discontinuous change in the molar volume [1, 2, 3, 4]. Such a first order transition can lead to phase coexistence of metallic and insulating states, where the length scales of these states are determined by strain and stress. In (La,Sr)MnO<sub>3</sub> and (La,Ca)MnO<sub>3</sub> [5] such phase coexistence has been observed for low concentrations of the divalent cation as droplets, and it results from competition between the 'potential' and 'kinetic' energy of the valence electron system. Electron delocalization is promoted by kinetic energy, whereas localization is promoted by the Coulomb repulsion between electrons. In manganite systems extremely diverse types of phase separation can develop, occurring on a variety of length-scales that can range from micrometers down to a few nanometers. Interestingly, phase coexistence not associated with metal-insulator transitions has also been observed; it can also arise from competition between different charge- and orbitally-ordered or disordered phases [6, 7]. The spin, charge and orbital orderings found in the manganites are often associated with large displacements of the ions in the lattice or even with changes in the molar volume. Generally, the orbital and charge ordering take place at higher temperatures than the magnetic ordering [8]. In both cases the coupling between the different phases is mediated through coupling with the lattice. In contrast, the coupling of orbital and spin-order is mostly of electronic nature by the antisymmetrization requirement of the wavefunction. In LaMnO<sub>3</sub> [9] the orbital interactions between the  $e_g$  electrons are much stronger ( $T_{o.o} \sim 800\text{K}$ ) than the magnetic interactions ( $T_N \sim 150\text{K}$ ). In contrast, the Jahn-Teller active  $t_{2g}$  electrons in the vanadates orbitally order at  $T_{o.o} \sim 200\text{ K}$  or lower. Although the difference between the spin and orbital ordering temperatures in the vanadates is smaller than that in the manganites, relatively little interaction between the spin and orbitally ordered states is observed. The orbital ordering temperature is higher than the magnetic ordering with the exception of LaVO<sub>3</sub>. For the small ionic size R in RVO<sub>3</sub>, complex behavior has been observed in which different types of orbital ordering occur [10, 11]. Here, a change in the orbital structure is accompanied by a change in spin order. This indicates a strong coupling between the two types of order as

required by the antisymmetric nature of the electron wavefunction, including spin and orbit. Nevertheless, the orders originate at distinctly different temperatures. Here, we report the orbital ordering of  $\text{SmVO}_3$ , in which coexistence of orbital orderings of different symmetry is triggered by magnetic ordering of the vanadium spins. This coexistence of orbital orderings is not associated with metal-insulator transitions, but is the result of magnetic exchange striction, which provides the coupling to the lattice.

Polycrystalline powder samples of  $\text{SmVO}_3$  were prepared by chemical reduction of  $\text{SmVO}_4$  at  $1400^\circ\text{C}$  under a  $\text{H}_2/\text{N}_2$  atmosphere. The  $\text{SmVO}_4$  powders were prepared by solid state reaction, using pre-dried  $\text{Sm}_2\text{O}_3$  (99.9%), and a 10% excess of  $\text{V}_2\text{O}_5$  (99.95%) to compensate the V-volatility. The sample shows a small impurity of  $\text{V}_2\text{O}_3$  due to the large excess of  $\text{V}_2\text{O}_5$  in the starting material. The high resolution X-Ray powder diffraction experiments were carried out on beamline ID31 at ESRF in Grenoble. During cooling down to 5K, short scans were performed. The temperature was then stabilized at 5K, and a long scan was measured. Then, short scans up to 254K were measured, while heating to room temperature (RT). The powder diffraction patterns were analyzed by the Rietveld method [12] using the refinement program GSAS [13] as implemented in the EXPGUI package [14]. The specific heat was measured between 3 and 300K using a relaxation method in a commercial Quantum Design Physical Properties Measurement System.

$\text{SmVO}_3$  has an orthorhombic perovskite structure at room temperature, as is common for all  $\text{RVO}_3$ , with R a rare earth element or Yttrium. The structure consists of corner sharing oxygen octahedra. The vanadium is located in the center of the octahedron, and the samarium is located between the octahedra. We could index the peaks belonging to the  $\text{SmVO}_3$  phase with the orthorhombic  $\text{Pbnm}$  space group. From the refinement of the diffraction pattern, we observed that  $\text{SmVO}_3$  stabilizes in an O-Orthorhombic structure at room temperature [15] ( $a < c/\sqrt{2} < b$ ) because of the buckling of the corner-shared octahedra [16].  $\text{SmVO}_3$  retains its orthorhombic structure down to  $T_{o.o}=200\text{K}$ . Here the symmetry changes to monoclinic  $\text{P2}_1/\text{b11}$ [25] as evidenced by the splitting and broadening of the diffraction lines. We identify this change in symmetry with the orbital ordering transition. This is confirmed by the specific heat measurement, as shown in Fig.1, and is consistent with other reports [11]. The value of the monoclinic angle increases slowly from  $90.00^\circ$  at 200K down to  $90.019(4)^\circ$  at 129K (Fig.2). As the temperature further decreases, the value of alpha increases rapidly to a maximum value of  $90.131(1)^\circ$  below 50K (Fig.1).

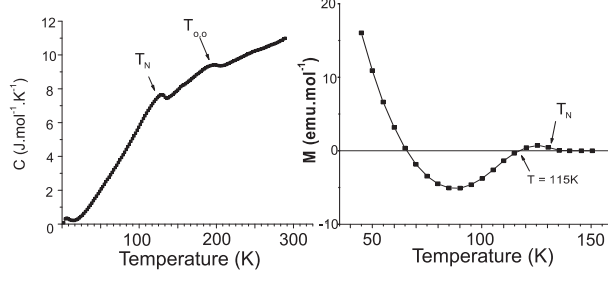


FIG. 1: Specific heat of  $\text{SmVO}_3$  (left) and temperature dependence of magnetization (measured in 1kOe) (right).

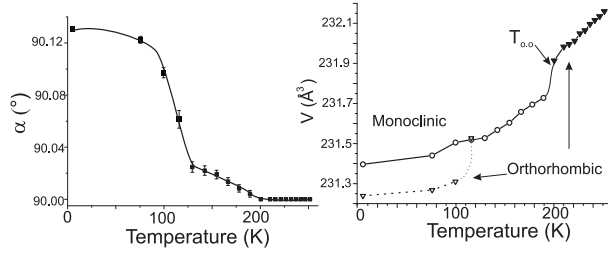


FIG. 2: Temperature dependence of the alpha angle (left), and of the unit-cell volume (right) in  $\text{SmVO}_3$ .

The onset of orbital ordering is accompanied by a change in the unit-cell volume (Fig.2). This monoclinic phase persists from the  $T_{o.o}$  down to the magnetic transition at  $T_N$  (Fig.3(b)), which is observed by both specific heat and magnetization measurements (Fig.1).

Below 115K we observe a coexistence of phases with monoclinic ( $P2_1/b11$ ) and orthorhombic ( $Pbnm$ ) symmetries, which remains down to our lowest measurement temperature of 5K (Fig.3(c)). The proportion of orthorhombic phase increases from 15% at 115K to 25% at 5K. Similar ratios were observed both upon cooling and warming the sample. We note that the phase coexistence sets in continuously below 115K, where both phases have the same molar volume. The V-O1, V-O2 and V-O3 distances, where O1 are the out-of plane and O2 and O3 are the in-plane oxygens, are important indicators of the type of orbital ordering of a system. In our data they are difficult to determine accurately because Sm, a heavy rare-earth, dominates the diffraction pattern and also because there is considerable overlap of peaks from the coexisting phases at low temperatures. However, as shown in Table I, the V-O distances confirm that the RT structure is not orbitally ordered and strongly suggest that at 5K both the monoclinic and orthorhombic phases are orbitally ordered. The V-O

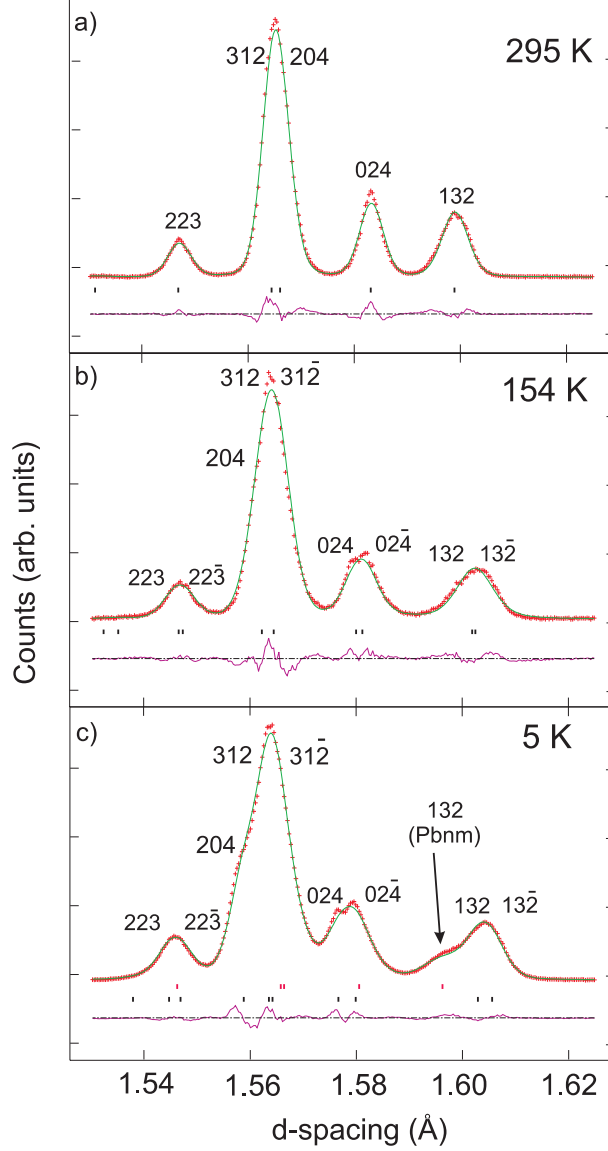


FIG. 3: Section of the diffraction pattern that shows the successive phases observed for  $\text{SmVO}_3$  with a):  $T > T_{o.o}$ : Pbnm ( $R_{wp}=0.078$ ), b):  $T_N < T < T_{o.o}$ :  $P2_1/b11$  phase, c):  $T < T_N$ : Pbnm (top markers) and  $P2_1/b11$  (bottom markers) phases ( $R_{wp}=0.0517$ ).

distances in the monoclinic and orthorhombic phases are comparable within error bars to those in the so-called G-type and C-type orbitally ordered phases of  $\text{YVO}_3$ , respectively [23]. A full list of refined atomic parameters, bond lengths and angles is deposited in the auxiliary material. To confirm the nature of these phases over the whole temperature range, since the rapidly collected cooling/heating data do not allow a precise determination of the oxygen fractional coordinates[26], we have chosen the lattice parameter ratio  $b/a$  (Fig.4) as

	5K (Pbnm)	5K (P2 <sub>1</sub> /b11)	295K (Pbnm)
V1-O1	2.026(5)	1.996(15)	1.9942(12)
V1-O2	1.977(12)	1.973(16)	2.0236(35)
V1-O2	2.025(12)	2.070(14)	2.008(34)
V2-O1		1.934(15)	
V2-O3		2.024(13)	
V2-O3		2.049(16)	

TABLE I: V-O bondlengths ( $\text{\AA}$ ) for  $\text{SmVO}_3$  in the orbitally ordered phases at 5K and non-ordered phase at 295K.

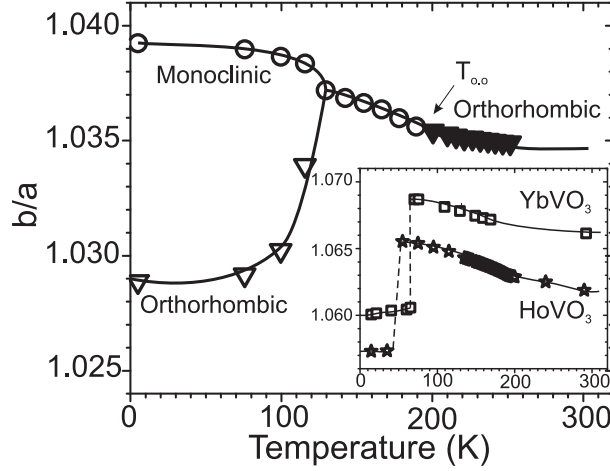


FIG. 4: Temperature dependence of the lattice parameter ratio  $b/a$  in  $\text{SmVO}_3$ : the filled triangles represent the orthorhombic phase above  $T_{o,o}$ ). The inset presents this ratio for other  $\text{RVO}_3$  with  $\text{R}=\text{Ho}$  (stars) and  $\text{Yb}$  (squares).

an indicator of the type of orbital ordering and compared it to the ratios for other  $\text{RVO}_3$  [17]. This comparison provides further evidence that the low temperature orthorhombic phase of  $\text{SmVO}_3$  is also orbitally ordered. For  $\text{YVO}_3$  [23],  $\text{HoVO}_3$  and  $\text{YbVO}_3$ , the transition from G- to C-type orbital ordering is discontinuous first order and a large drop of the  $b/a$  ratio can be observed. Moreover, it occurs at much lower temperature than the magnetic ordering. In contrast, for  $\text{SmVO}_3$  the transition is continuous and is observed to set in very close to  $T_N$ .

The type of orbital ordering (OO) present in the ground state of the  $\text{RVO}_3$  compounds

depends mainly on the degree of octahedral tilting caused by the deviation in size of the rare-earth cation from that in the ideal cubic perovskite. Although all  $\text{RVO}_3$  compounds initially order in the so-called G-type structure ( $d_{xy}d_{yz}$  and  $d_{xy}d_{xz}$  orbitals are occupied alternately along all three directions of the lattice), on increasing the octahedral tilting as the rare-earth cation becomes smaller a first-order transition to a C-type OO ground state ( $d_{xy}d_{yz}$  and  $d_{xy}d_{xz}$  orbitals are occupied alternately in the  $ab$  plane while the same orbitals are occupied along  $c$ ) occurs in the range 50 K to 80 K for rare-earths smaller than Tb [11]. This phase transition involves a large decrease in unit cell volume. In these strongly distorted structures, the C-type ground state is largely stabilized by a shift of the R cation in order to maximize the R-O covalency [10, 18].

$\text{SmVO}_3$  lies far into the G-type OO region of the phase diagram. As observed in both our specific heat and diffraction measurements, G-type OO takes place in  $\text{SmVO}_3$  at 200 K and the resulting monoclinic distortion becomes progressively larger with decreasing temperature, as indicated by the monoclinic angle,  $\alpha$ , shown in Fig.2. However, below 105 K the value of  $\alpha$  shows a rapid increase before reaching a constant value below 50 K. More surprisingly, 15% of the sample is transformed into the C-type OO structure in the vicinity of  $T_N$ . This C-type phase persists on further cooling with a fraction that gradually increases to 25% at 5 K. Both the appearance of the C-type phase and the rapid increase in the monoclinic distortion of the G-type phase are most likely associated with the onset of magnetic ordering.

It has long been known that a structural distortion, known as magnetic exchange striction, can occur at or shortly below  $T_N$  in transition metal oxides in order to increase the magnetic exchange interaction energy [19]. This type of distortion has previously been observed in  $\text{LaVO}_3$  [20, 21] and  $\text{CeVO}_3$  [20]. In the case of  $\text{CeVO}_3$  the type of OO remains the same, but the exchange striction occurring at  $T_N$  involves a small increase in  $a$  and  $b$ , a large decrease in  $c$ , and an overall decrease in the unit cell volume. In the case of  $\text{LaVO}_3$ , G-type OO arises 2 K below the magnetic ordering temperature and may itself be the result of exchange striction. However, in the "small radius"  $\text{RVO}_3$  compounds such as  $\text{YVO}_3$ , the structural change at  $T_N$  is tiny [22]. The difference between the orbital and magnetic ordering temperatures in these compounds is much greater than in  $\text{LaVO}_3$  and  $\text{CeVO}_3$  [11] and V-O bond lengths suggest that orbital ordering is fully developed at  $T_N$  [10]. Therefore, there is little further energy to be gained through a structural distortion.

The exchange striction occurring at  $T_N$  in  $\text{SmVO}_3$  is expected to be intermediate in magnitude between that in  $\text{CeVO}_3$  and  $\text{YVO}_3$ ; the large increase in the monoclinic angle  $\alpha$  below  $T_N$  (Fig.1) suggests that orbital ordering in the G-type phase is incomplete at this point. Since the exchange striction appears to cause a volume decrease, one may expect the onset of magnetic ordering to promote the C-type phase; that is, the C-type phase will be lowered in energy to an extent that depends on the magnitude of the exchange striction. For compounds such as  $\text{CeVO}_3$  the G-type phase is much lower in energy at all temperatures due to the smaller degree of octahedral tilting. At the other end of the phase diagram the exchange striction in the G-type phase at  $T_N$  is too weak to have any effect on the crystal structure. However, for materials closer to the phase boundary such as  $\text{SmVO}_3$ , the exchange striction is still significant and may be strong enough to lower the energy of the C-type phase enough to become favored.

Somewhat surprisingly, in  $\text{SmVO}_3$  the unit cell volumes of the two OO phases are equal (at the precision of our diffraction measurements) immediately below  $T_N$  (Fig.2). However, this can be explained by a scenario where small droplets of the C-type phase are initially formed in a G-type matrix. Although the C-type droplets can be distinguished by X-ray diffraction, implying coherent OO over length-scales of at least several hundred angstroms, they are still relatively small and isolated compared to the surrounding G-type phase. The unit cell volume of regions of a droplet close to an interface will be forced to match that of the surrounding matrix and large strain fields will thus extend throughout droplets that are small. On further cooling, the C-type droplets will tend to enlarge and coalesce into domains big enough for relaxation of the strain to take place. This relaxation is seen in the rapid decrease of the unit cell volume as the fraction of the C-type phase grows. However, the remaining strain might still be large enough to inhibit further transformation of the G-type matrix, stabilizing the phase-separated state with little change in phase fractions below 80 K. The difference in unit cell volumes of the two phases at 5 K is 0.067%, which can be compared to changes of 0.16% on cooling through the first-order transition in  $\text{YVO}_3$  [23], 0.15% in  $\text{HoVO}_3$  and 0.16% in  $\text{YbVO}_3$  [17], where full transformation to the C-type phase is achieved. The suppressed volume decrease in  $\text{SmVO}_3$  is further evidence that significant strain remains in the system down to 5 K.

Although specific heat measurements show no transition between orbital orderings below  $T_N$  in other "intermediate radius" vanadates such as  $\text{EuVO}_3$ ,  $\text{GdVO}_3$  and  $\text{TbVO}_3$  [11], the



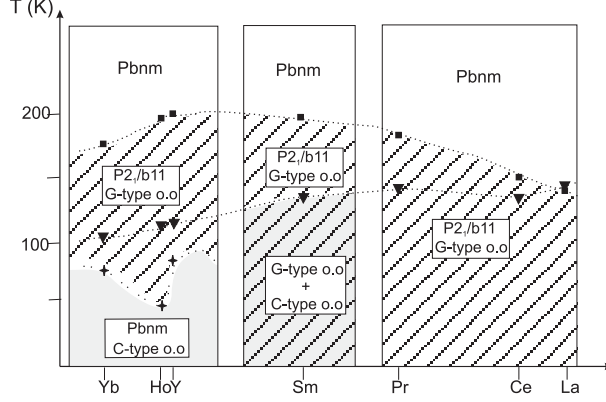


FIG. 5: Phase diagram obtained for  $\text{RVO}_3$  studied by diffraction techniques. The squares represent the onset of orbital ordering, the triangles represent spin ordering, stars represent the first order transition.

low-temperature phase composition of these materials has thus far not been studied by techniques such as high resolution X-ray diffraction. It remains to be seen whether these materials will also display phase separation between the two types of OO. On one hand the tendency towards C-type OO increases with smaller rare-earth radius, but on the other hand the exchange striction at  $T_N$  that appears to promote transformation to the C-type phase is expected to decrease in magnitude. Nevertheless, it is likely that the border between the C- and G-type phases as a function of ionic radius is not a sharply defined line, as suggested by the phase diagram of Miyasaka et al. [11], but rather occurs via a broad phase separated region.

We propose a modified  $\text{RVO}_3$  phase diagram in Fig.5 based on diffraction data. For small rare-earths such as Yb, Ho and Y, complete transformation from G-type to C-type OO is achieved on cooling through a first-order transition well below  $T_N$ . For large rare-earths such as La, Ce and Pr [24] the orbital ordering remains of G-type down to at least 5 K. However, for intermediate rare-earths such as Sm, a region of coexistence between C-type and G-type phases is present at all temperatures below  $T_N$ . In summary, high resolution X-ray diffraction has demonstrated that vanadium spin ordering in  $\text{SmVO}_3$  induces magnetic exchange striction that changes the symmetry of the orbital ordering in part of the sample. The two types of orbital ordering then coexist down to low temperature, a situation that is stabilized purely by lattice strains associated with the difference in unit cell volumes of the two phases.

We thank Dr. I. Margiolaki for experimental assistance at ESRF and for useful discussions on the X-Ray diffraction experiments. We are grateful to Prof. D.I. Khomskii for enlightening and stimulating discussions. We acknowledge financial support by the European project SCOOTMO RTN (Contract No. HPRN-CT-2002-00293).

---

\* Corresponding author, email: t.t.m.palstra@rug.nl

- [1] Y. Tokura and Y. Tomioka, J. Magn. Magn. Mater. **200**, 1 (1999).
- [2] E. Dagotto, T. Hotta and A. Moreo, Phys. Rep. **344**, 1 (2001).
- [3] E. L. Nagaev, *Colossal magnetoresistance and phase separation in magnetic semi-conductors* (Imperial College Press, London, 2002).
- [4] C. Sen, G. Alvarez and E. Dagotto, Phys. Rev. B **70**, 064428 (2004).
- [5] J. C. Loudon, N. D. Mathur and P. A. Midgley, Nature **420**, 797 (2002).
- [6] P. G. Radaelli *et al.*, Phys. Rev. B **63**, 172419 (2001).
- [7] J. P. Chapman *et al.*, Dalton Trans. **19**, 3026 (2004).
- [8] Y. Murakami *et al.*, Jpn. J. Appl. Phys. **38**, 360 (1999).
- [9] Y. Murakami *et al.*, Phys. Rev. Lett. **81**, 582 (2005).
- [10] G. R. Blake *et al.*, Phys. Rev. Lett. **87**, 245501 (2001).
- [11] S. Miyasaka, Y. Okimoto, M. Iwama and Y. Tokura, Phys. Rev. B **68** (2003).
- [12] H. M. Rietveld, J. Appl. Cryst. **2**, 65 (1969).
- [13] A. C. Larson and R. B. von Dreele, Los Alamos Laboratory Report No LAUR 86-748 (1994).
- [14] B. H. Toby, J. Appl. Cryst. **34**, 210 (2001).
- [15] J. B. Goodenough and J. M. Longo, *Crystallographic and Magnetic Properties of Perovskite and Perovskite-Related Compounds*, in Landolt-Bornstein Tabellen, New Series III/4a, edited by K.-H. Hellwege, (Springer-Verlag, Berlin, 1970), Chap. 3, p. 126.
- [16] A. M. Glazer, Acta Crystallogr. A **31**, 756 (1975).
- [17] G. Blake *et al.*, to be published.
- [18] T. Mizokawa, D. I. Khomskii and G. A. Sawatzky, Phys. Rev. B **60**, 7309 (1999).
- [19] S. Greenwald and J. S. Smart, Nature **166**, 523 (1950).
- [20] Y. Ren *et al.*, Phys. Rev. B **67**, 014107 (2003).
- [21] P. Bordet *et al.*, J. Solid State Chem. **106**, 253 (1993).

- [22] C. Marquina *et al.*, J. Magn. Magn. Mater. **290-291**, 428 (2005).
- [23] G. R. Blake *et al.*, Phys. Rev. B **65**, 174112 (2002).
- [24] M. H. Sage *et al.*, to be published.
- [25] We use  $P2_1/b11$  for the monoclinic phase instead of the standard setting  $P2_1/c$  in order to allow a direct comparison of the lattice parameters, Miller indices and atomic coordinates of the monoclinic phase with those of the orthorhombic  $Pbnm$  phases.
- [26] These datasets were collected over 5-10 minutes and, although sufficient for a precise determination of the lattice parameters, cell volume, monoclinic angle and phase fractions, below  $T_{OO}$  the accurate determination of oxygen fractional coordinates was not possible; the atomic parameters were thus fixed to those determined for the  $P2_1/b11$  and  $Pbnm$  phases at 5K.